

Enhancing Water Quality Through the Sorptive Removal of Malachite Green Dye from Aqueous Solution Using Magnesia

Lerato Khoza¹, Tholiso Ngulube¹, and Mabel Mphahlele-Makgwane¹

Abstract—The widespread use of synthetic dyes like Malachite Green (MG) in industries such as textiles and aquaculture has led to significant environmental pollution. MG is toxic, mutagenic, and potentially carcinogenic, necessitating effective removal methods to protect water resources. This study explored using magnesia (MgO) as an adsorbent to remove MG from aqueous solutions, optimizing adsorption parameters like adsorbent dosage, contact time, dye concentration, and pH. MgO, with its high surface area and active sites, showed effective adsorption capabilities. Characterization using X-ray Fluorescence (XRF), Scanning Electron Microscopy (SEM), and Fourier Transform Infrared Spectroscopy (FTIR) revealed significant structural and chemical changes in MgO before and after adsorption. The optimal conditions for MG removal were 1.7 g of MgO, 5 minutes of contact time, a dye concentration of 60 mg/L, and a pH of 5. The removal efficiency met SANS 241 water quality standards, demonstrating MgO as a low-cost, sustainable solution for mitigating dye pollution in industrial wastewater.

Keywords— Adsorption, Magnesia, Malachite Green Dye, Water Quality

I. INTRODUCTION

South Africa is a water scarce country. It ranks as one of the 30 driest countries in the world with an average rainfall of about 40% less than the annual world average rainfall [6]. As South Africa's population continues to grow and the economy expands, millions of people still lack access to essential services. It is now believed that the demand for water matches or even exceeds the available supply [5]. Water is the foundation of our economy, playing a crucial role in agriculture, industries, recreation, and domestic uses. Ensuring safe and sufficient water supplies is vital for sustaining these sectors. The textile industry is recognized as the second-highest industrial activity in terms of water consumption, following agricultural practices, due to its vast water usage across various production phases [8]. Over 50% of the water input in the textile industry's dyeing process is consumed, producing significant amounts of effluents

Lerato Khoza¹ is with the University of Limpopo, Department of Water and Sanitation Private Bag x1106, Sovenga, 0727, South Africa

Tholiso Ngulube¹, is the University of Limpopo, Department of Water and Sanitation Private Bag x1106, Sovenga, 0727, South Africa

Mabel Mphahlele-Makgwane¹ is with the University of Limpopo, Department of Water and Sanitation Private Bag x1106, Sovenga, 0727, South Africa

primarily composed of unfixed dyes [3]. Synthetic dyes, such as MG, are extensively employed in the production of paints, fabrics, printing inks, medicines, food, cosmetics, plastics, photography, and paper products due to their wide range of colors and cost-effectiveness [5].

The discharge of dye-laden wastewater from textile industries has severe impacts on aquatic ecosystems and poses health risks to humans [2]. Many synthetic dyes and their degradation products are toxic and carcinogenic, causing issues such as skin dysfunction, respiratory irritation, and eye allergies. Even in small amounts, dyes in water compromise water quality by limiting light penetration, inhibiting photosynthesis, reducing oxygen levels, and restricting water's use for activities like irrigation and drinking [7]. Ensuring optimal water quality is essential for human health, ecosystem resilience, and biodiversity, highlighting the importance of managing natural and anthropogenic influences on water quality.

MG a commonly used dye in textiles and laboratory staining, poses significant environmental and health risks. It can accumulate in tissues of animals and humans, potentially causing long-term health hazards [4]. MgO has shown promise as a low-cost, effective adsorbent for removing MG from water, utilizing electrostatic interactions, hydrogen bonding, and Van der Waals forces to capture dye molecules. Researchers are working to optimize MgO-based adsorption techniques to improve removal efficiency, addressing the environmental threat posed by dye pollution [1].

II. MATERIALS AND METHODS

A. Sampling

The study was conducted at the Capricorn District Municipality labs at the University of Limpopo. MgO was purchased from Strathmore Magnesite, a mining company in Malelane, South Africa. MG was purchased from Lasec Pty Ltd, South Africa. The study is lab based, it does not have a study area.

B. Preparation of MG Dye Solution

An analytical balance was used to accurately weigh 1 g of MG dye. The 1 g of MG dye was transferred into a 1000 mL volumetric flask. Then, 10 mL of distilled water was added to the flask, and the mixture was swirled gently until the dye was

completely dissolved. Once fully dissolved, the volumetric flask was filled with distilled water up to the 1000 mL mark. The flask was capped and inverted several times to ensure thorough mixing. Finally, the flask was labelled as "MG Stock Solution, 1000 mg/L."

C. Batch Adsorption Experiments

Six, 120 mL beakers were labelled for each set of conditions planned for testing, including contact time, adsorbent dosage, dye concentration, and pH. The required amounts of MgO (adsorbent) were weighed, ranging from 0.5, 0.8, 1.1, 1.4, 1.7, to 2 g for each experiment using an analytical balance. Then, 100 mL of a 10 mg/L MG solution was added to each beaker. The weighed MgO was added to each beaker containing the MG dye solution. The beakers were placed on a stirrer set to 200 rpm for 5 minutes, then centrifuged for 15 minutes at 4000 rpm. The absorbance of each sample was measured at 614 nm using a UV-Vis spectrophotometer. This experiment was conducted in triplicate for quality assurance.

Next, contact time was varied for 5, 15, 30, 45, 60, and 90 minutes using the optimal adsorbent dosage in six beakers containing the MG dye solution. The beakers were stirred at 200 rpm for 5 minutes, then centrifuged for 15 minutes at 4000 rpm. The absorbance of each sample was measured at 614 nm using a UV-Vis spectrophotometer. The experiment was repeated two more times to determine the optimal contact time.

To determine the volume of the stock solution needed for each target concentration the dilution formula

$$C_1V_1=C_2V_2$$

... (1) was used. In six beakers, different concentrations (10 mg/L, 30 mg/L, 60 mg/L, 90 mg/L, 120 mg/L, 150 mg/L), of MG dye solution were prepared with the optimal dosage and stirred at the optimal contact time, then centrifuged for 15 minutes at 4000 rpm. The absorbance of each sample was measured at 614 nm using a UV-Vis spectrophotometer. The experiment was done in triplicate to determine the optimal concentration.

Finally, the pH of the solutions was adjusted to 1, 3, 5, 7, 9, and 11 using pH adjusters (HCl for acidic conditions and NaOH for basic conditions). In six beakers, the optimal dye concentration of MG dye solution was added with the optimal dosage and stirred at the optimal contact time in the different pH solutions, then centrifuged for 15 minutes at 4000 rpm. The absorbance of each sample was measured at 614 nm using a UV-Vis spectrophotometer. The experiment was performed in triplicate to determine the optimal pH. The MgO sludge was then dried in the oven at 105°C for an hour and taken for characterization.

D. Characterization Studies

SEM Analysis

The morphology of the MgO samples before and after treatment was examined using a Sigma FE-SEM (USA). The samples were mounted on stubs with carbon tape, placed in

the SEM chamber, and coated with a thin layer of gold to make them conductive. Various detectors captured the signals, producing image that revealed the characteristics of the sample.

XRF Analysis

Bruker XRF spectrometer was used to analyse the major and minor elements in MgO before and after treatment.

FTIR Analysis

MgO samples before and after treatment were analyzed by FTIR using a flow-through continuous reactor. The infrared spectra in the mode were recorded in the 4000-400 cm^{-1} frequency region using a Bruker Tensor 27 spectrometer. The measurements of bands integrated intensity were made using OPUS software supplied by Bruker instrument.

Calculation Of % Adsorption And Adsorption Capacity Of MG Dye

Equation 2 was used calculate the percentage removal of MG:

$$\% \text{Removal} = ((C_0 - C_f) / C_0) \times 100 \quad (2)$$

Where C_0 is the initial concentration and C_f is the final concentration after adsorption.

Equation 3 was used to calculate the adsorption capacity Q_e :

$$Q_e = (C_i - C_e)V/M \quad (3)$$

Where C_i is the initial concentration, C_e is the equilibrium concentration, V is the volume of the solution, and M is the mass of the adsorbent.

500 mL of AMD solution was added into 6, 1000 mL beakers and 1 g, 3 g, 5 g, 10 g, 15g, and 20 g of CaO was added to each beaker. Then the mixtures were agitated for 10 minutes at 200 rpm using a 4-paddle stirrer (Model 1924, Electronics, India). The experiments were carried out in triplicate at room temperature of 25°C.

III. RESULTS AND DISCUSSIONS

A. Adsorption Studies

Variation Of Dosage

Fig.1. illustrates the effect of MgO dosage on the percentage removal of Mg dye (% Removal) and the adsorption capacity (Q_e) at different dosages ranging from 0.5 g to 2 g.

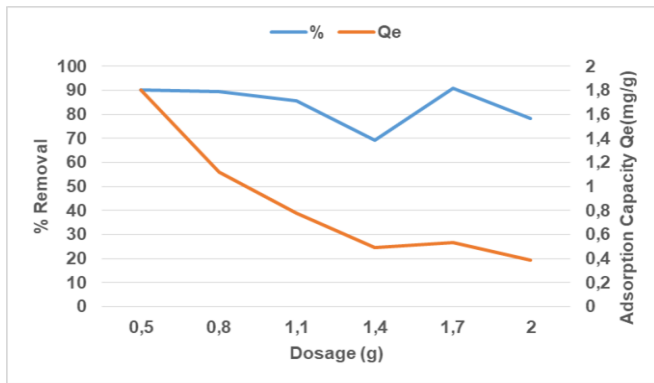


Fig.1. Variation of dosage on percentage removal (% Removal) and adsorption capacity (Qe (mg/g)) of MG dye using MgO as the adsorbent.

Fig.1. illustrates that the percentage removal of dye initially remains high at low MgO dosages, around 90% at 0.5 g, but gradually declines with increased dosage. As the dosage increases to 1.4 g, the removal efficiency drops to 69.2%, likely due to temporary saturation of active adsorption sites. At higher dosages, particle aggregation may reduce the available surface area, limiting adsorption effectiveness. The removal efficiency rises again to 90.8% at 1.7 g, possibly due to re-equilibration, before slightly declining as near-saturation is reached at 2.0 g. These trends indicate the complex balance between dosage and adsorption site utilization.

The adsorption capacity (Qe) per gram of MgO decreases sharply with increasing dosage, as more MgO particles provide excess surface area that remains unused due to fewer dye molecules available per unit mass of adsorbent. This decrease in Qe highlights that while higher dosages enhance overall dye removal, they reduce the efficiency of dye uptake per gram of MgO, emphasizing the need for dosage optimization. Thus, achieving cost-effective water treatment requires balancing dosage levels to maximize both dye removal and adsorption efficiency.

Variation of Contact Time

Fig. 2 illustrates the effect of contact time on the percentage removal of MG dye and adsorption capacity over a period ranging from 5 to 90 minutes.

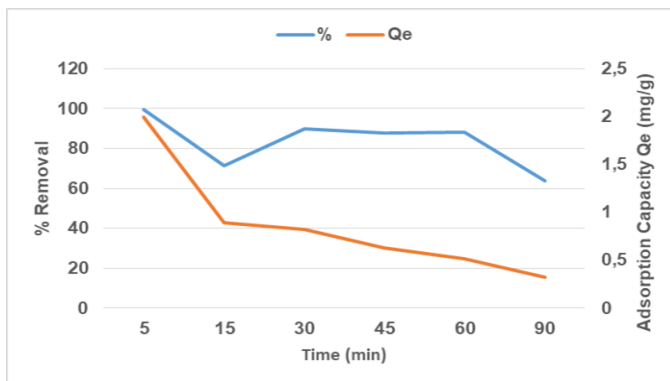


Fig.2. Variation of time on percentage removal (% Removal) and adsorption capacity (Qe) of MG dye using MgO as the adsorbent.

Fig.2. shows that dye adsorption onto MgO is rapid initially, with percentage removal reaching around 90% at 5 minutes due to abundant active sites. However, after 15 minutes, the removal drops significantly to 71.52% as these sites are quickly occupied. At 30 minutes, removal efficiency rebounds to 90.03%, indicating a stabilization phase as equilibrium approaches. Minimal fluctuations between 45 and 60 minutes suggest equilibrium has nearly been achieved, with additional contact time providing little improvement. By 90 minutes, a decline to 63.69% removal suggests potential desorption or competition for sites. The steady decrease in adsorption capacity (Qe) over time reinforces the need to optimize contact time for effective dye removal in water treatment applications using MgO.

Variation of Dye Concentration

In Fig.3. adsorption of MG dye onto MgO was investigated at varying dye concentrations ranging from 10 to 150 mg/L.

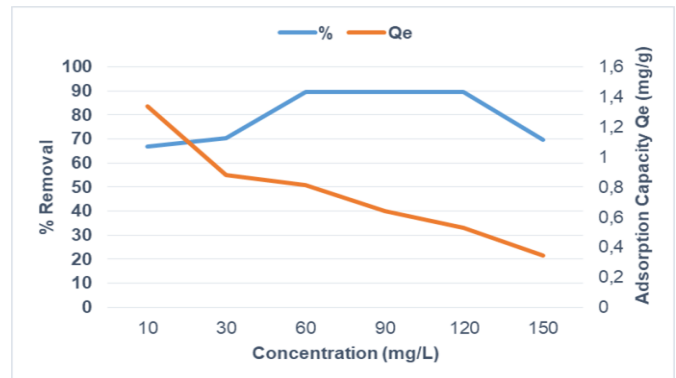


Fig.3. Variation of concentration on percentage removal and adsorption capacity of MG dye using MgO as the adsorbent.

The study analyzed how varying initial concentrations of MG dye (10 to 150 mg/L) affected the percentage removal and adsorption capacity (Qe) of MgO. Results indicated a non-linear trend in removal efficiency: it increased from 66.99% at 10 mg/L to a peak of 89.64% at 60 mg/L, stabilizing around this level at moderate concentrations (90 to 120 mg/L) before dropping to 69.54% at 150 mg/L. This pattern suggests MgO is highly effective at moderate dye concentrations, but removal efficiency diminishes at the highest concentration due to limited adsorption sites.

The adsorption capacity (Qe) showed a consistent decline with rising dye concentration, starting at 1.34 mg/g at 10 mg/L and dropping to 0.35 mg/g at 150 mg/L. This decline is likely due to saturation of active sites on MgO at higher concentrations, where fewer sites are available per dye molecule. These findings suggest that the adsorption process is more efficient at lower dye concentrations, where a higher adsorbent-to-dye ratio enhances dye uptake per unit mass of MgO, emphasizing the importance of concentration in optimizing dye removal efficiency.

Variation of pH

In Fig.4. the adsorption behaviour of MgO was also studied across a wide pH range (1-11) to assess its impact on MG dye removal efficiency and adsorption capacity.

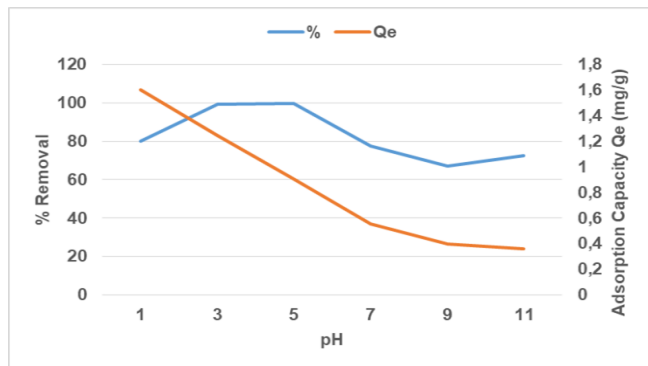


Fig.4. Variation of pH on percentage removal and adsorption capacity of MG dye using MgO as the adsorbent.

pH significantly influences the adsorption of MG dye onto MgO by affecting the surface charge of MgO and the dye's ionization state. The highest removal efficiency (99.71%) occurred in a mildly acidic environment at pH 5, with

similarly high efficiency at pH 3 (99.39%). Adsorption efficiency declined sharply in alkaline conditions, with the lowest values at pH 9 (67.21%) and pH 11 (72.36%), likely due to increased negative surface charge on MgO, reducing electrostatic attraction to the cationic dye. Although adsorption capacity (Q_e) was highest at pH 1 (1.60 mg/g), it declined as pH increased, reaching a minimum of 0.36 mg/g at pH 11. These findings underscore the importance of maintaining slightly acidic conditions for optimal dye removal.

B. Comparison of MG Treated Water with SANS Industrial Water Quality Standards

Table 1 illustrates the comparison between the treated MG water and the SANS (South African National Standards) water quality standards, highlighting key parameters. The optimum conditions for treating MG were found to be an adsorbent dosage of 1.7 g, a contact time of 5 minutes, an initial dye concentration of 60 mg/L, and a pH of 5. These optimized conditions allowed for an effective removal of the dye, as well as improvements in other water quality indicators.

TABLE I
COMPARISON OF MG TREATED WATER WITH SANS WATER QUALITY STANDARDS (OPTIMIZATION CONDITIONS)

Parameter	SANS Industrial Standard	MG Treated Water	Discussion
Colour	None	None	The treated water meets the SANS standard, showing no colour indicating efficient dye removal.
pH	5.5-8.5	5.8	The pH falls within the acceptable range, showing that the treatment maintained pH balance without altering water properties.
Turbidity	3 NTU	0.7 NTU	Turbidity is significantly lower than the standard, indicating excellent removal of suspended particles and improved water clarity.
Temperature	35° C	27° C	The temperature of the treated water is lower than the standard, which should not negatively impact industrial use and may be beneficial.
Electrical Conductivity	75 mS/m	43 mS/m	The treated water shows reduced conductivity, suggesting effective removal of dissolved ions, lowering the risk of scaling and corrosion.

The optimized conditions demonstrated high effectiveness in treating water as it met the SANS industrial water quality standards. The complete removal of color eliminated aesthetic concerns, while the treated water's pH of 5.8 remained within the safe range of 5.5–8.5. With a low turbidity of 0.7 NTU, well below the 3 NTU limit, and a temperature of 27°C, below the SANS maximum of 35°C, the water was clear and

safe for industrial use. The conductivity of 43 mS/m, lower than the 75 mS/m standard, confirmed effective reduction of dissolved ions, making the treated water suitable for applications requiring low conductivity.

C. Characterization Results

XRF Analysis

Table II shows the elemental composition of the adsorbent material before and after the dye treatment process. The percentage composition of various elements, including MgO, Al_2O_3 , SiO_2 , and others, is listed to highlight changes in their concentrations following the adsorption of dye. Notably, MgO, which serves as the primary adsorbent, experiences a significant decrease in composition after dye treatment, while other elements show minor variations, reflecting their interaction or stability during the process. This data provides insight into the material's adsorption efficiency and elemental behaviour.

TABLE II
XRF DERIVED CHEMICAL COMPOSITIONS OF ELEMENTS IN MGO BEFORE AND AFTER TREATMENT.

Element name	% Composition before dye treatment	% Composition after dye treatment
MgO	41.172	30.224
Al_2O_3	0.288	0.006
SiO_2	5.208	3.653
P_2O_5	0.003	0.000
S	0.078	0.093
K_2O	0.048	0.064
CaO	1.075	0.962
TiO_2	0.162	0.146
V	0.019	0.016
MnO	0.015	0.013
Fe_2O_3	1.047	1.043

The elemental composition of MgO before and after treatment reveals changes in the presence and concentration of various elements, which provide insights into the material's characteristics and behaviour during the adsorption process. MgO before treatment was 41.172% then after treatment it was 30.224%. MgO is the primary component of the adsorbent and serves as the main active surface for the adsorption of pollutants such as MG dye. The decrease in MgO content after treatment suggests that some of the MgO may have been involved in interactions with the dye molecules or lost due to leaching during the adsorption process.

The interaction that may have occurred between MgO and the dye molecules during the adsorption process is surface complexation or chemisorption. MgO has a high surface reactivity due to its alkaline nature and the presence of Mg^{2+} ions. During adsorption, the dye molecules may interact with the Mg^{2+} ions on the MgO surface through electrostatic attraction or chemical bonding.

The reduction in SiO_2 content from 5.208% before treatment to 3.653% after treatment suggests that despite being less reactive than MgO, SiO_2 may have played a role in the adsorption process. While SiO_2 is typically present as an impurity in MgO, its involvement could occur through physisorption or weak interactions with the dye molecules.

SiO_2 , being a silicate, has a surface covered with hydroxyl

groups (-OH) that can participate in hydrogen bonding or Van der Waals interactions with polar dye molecules. These weak, non-covalent interactions may have contributed to some adsorption capacity of the dye onto the SiO_2 surface, leading to the reduction in its content after treatment. Additionally, SiO_2 might act as a secondary support, enhancing the overall surface area available for adsorption in conjunction with MgO, although its activity is significantly lower.

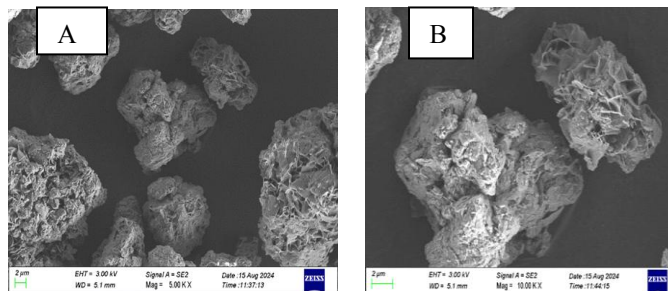
The decrease in SiO_2 content could also indicate that some of the silica may have been leached or dissolved during the treatment process, particularly under certain pH conditions, leading to a reduction in its overall concentration post-treatment. While its primary role in adsorption is minimal compared to MgO, SiO_2 may still contribute through these weaker physical interactions or be affected by the chemical environment during dye adsorption.

Al_2O_3 , present as an impurity in natural or industrial-grade MgO, shows a significant decrease from 0.288% before treatment to 0.006% after treatment. This substantial reduction suggests that Al_2O_3 may have been partially removed or dissolved during the adsorption process or washing steps, contributing to the further purification of the MgO. Fe_2O_3 , present as a trace impurity, shows minimal change in concentration, decreasing only slightly from 1.047% before treatment to 1.043% after treatment. While Fe_2O_3 can sometimes contribute to adsorption through electrostatic interactions, the negligible change suggests that Fe_2O_3 played a minimal role in the adsorption process in this case.

The XRF analysis shows that the elemental composition of MgO changes significantly during the adsorption process. The decrease in MgO, Al_2O_3 , and SiO_2 , suggest that MgO undergoes transformations or losses due to its interaction with malachite green dye. The stable presence of Fe_2O_3 and changes in sulfur highlight specific interactions or effects from the adsorption process.

SEM Analysis

The images for SEM micrographs are presented in Fig.5, which shows highly magnified images used to study the surface morphology and structure of materials at a microscopic scale. These images represent MgO material before and after the dye treatment process.



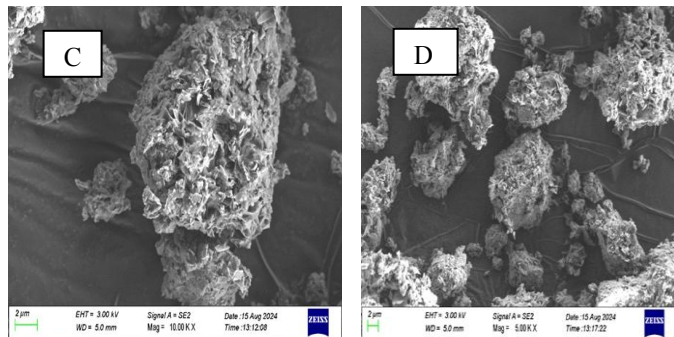


Fig.5. SEM images for A and B showing the surface morphology of MgO before dye treatment and image C and D showing the surface morphology of MgO after dye treatment.

In image A and B, the particles in the image have an irregular, rough surface with a clustered, porous appearance. These porous structures often indicate higher surface area, which is crucial for adsorption applications. Based on the scale bar, the particle size is in the range of 2-10 μm , which is typical for powdered or aggregated materials like MgO. The material looks to be untreated, indicating a potentially clean surface with no obvious signs of contaminants or reaction products.

The image C and D after treatment, the particles still appear aggregated but may exhibit surface changes. Some agglomerates look more compact or "smoother" compared to the rough and porous texture in Image A. This could indicate that the material underwent adsorption or surface reactions, possibly due to the capture of contaminants or pollutants during adsorption. Depending on the treatment process, the smoother surfaces might suggest that the surface is now coated with reaction byproducts or that some of the original surface roughness has been reduced by the treatment. The interaction between particles may be more evident in the post-treatment image. For example, particles might have formed more stable structures due to chemical or physical binding.

FTIR Analysis

Fig.6. depicts the FTIR spectra for MgO before and after treatment. FTIR is a common technique used to identify functional groups on the surface of materials by measuring the absorbance of infrared light at different wavelengths. In this case, the spectra help to analyse changes in surface functional groups on the MgO material during the treatment process.

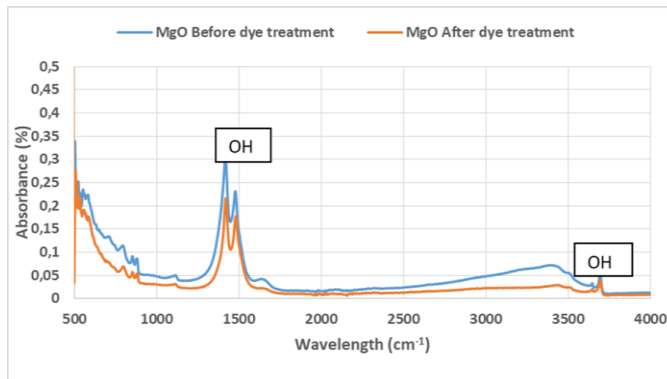


Fig.6. The FTIR graph before and after treatment of MG

Before treatment the strong peak near 1500 cm^{-1} corresponds to the OH stretching vibration, which indicates the presence of hydroxyl groups on the MgO surface. This could be related to moisture or surface-bound water. There is another significant OH-related peak around 3500 cm^{-1} , showing that the surface is rich in hydroxyl groups prior to treatment. These groups are typically associated with the surface of MgO, as it can adsorb water from the atmosphere or solution.

After treatment, the intensity of the peaks at 1500 cm^{-1} and 3500 cm^{-1} related to OH vibrations significantly decreased. The reduction in surface-bound hydroxyl ($-\text{OH}$) groups on MgO suggests that these groups may have played a significant role in the adsorption of the dye, particularly MG, during the treatment process. Hydroxyl groups are known to be reactive sites on the MgO surface, providing opportunities for interaction with polar or charged species, such as dye molecules [8].

In the case of MG, the dye has cationic properties, meaning it carries a positive charge in solution. The $-\text{OH}$ groups on MgO can form hydrogen bonds or electrostatic interactions with the positively charged amine groups in the dye molecule. When the MgO surface is rich in $-\text{OH}$ groups, these interactions facilitate the adsorption of the dye, enhancing removal efficiency.

However, the treatment process may have led to the removal or alteration of some of these hydroxyl groups, reducing the available reactive sites for dye interaction. As the treatment progressed, the adsorption of pollutants like MG could have replaced some of the $-\text{OH}$ groups on the surface, effectively blocking these sites. Consequently, this reduction in surface $-\text{OH}$ groups would diminish the MgO's ability to interact with the dye, ultimately impacting the overall adsorption capacity. Thus, the decrease in hydroxyl groups not only reflects changes in the surface chemistry of MgO but also indicates a potential mechanism through which the dye is adsorbed, highlighting the importance of these functional groups in the adsorption process.

ACKNOWLEDGMENT

The authors would like to acknowledge the Department of Water and Sanitation, University of Limpopo for providing

resources to make this research possible.

REFERENCES

- [1] Cui, Z., Liu, J., Gao, H., Xue, Y., Hao, J., Zhang, R., Ji, B. and Chen, J. Size and shape dependences of the adsorption kinetics of malachite green on nano-MgO: a theoretical and experimental study. *Physical Chemistry Chemical Physics*, 21(25), 2019, pp.13721-13729. <https://doi.org/10.1039/C9CP01279F>
- [2] Grover, A., Mohiuddin, I., Malik, A.K., Aulakh, J.S., Vikrant, K., Kim, K.H. and Brown, R.J. Magnesium/aluminum layered double hydroxides intercalated with starch for effective adsorptive removal of anionic dyes. *Journal of Hazardous Materials*, 424, 2022, pp.1274-1295. <https://doi.org/10.1016/j.jhazmat.2021.127454>
- [3] Guo, F., Jiang, X., Li, X., Jia, X., Liang, S. and Qian, L. Synthesis of MgO/Fe₃O₄ nanoparticles embedded activated carbon from biomass for high-efficient adsorption of malachite green. *Materials Chemistry and Physics*, 240, 2020, pp.1222-1240. <https://doi.org/10.1016/j.matchemphys.2019.122240>
- [4] Hasan, I.M.A., Salman, H.M. and Hafez, O.M. Ficus-mediated green synthesis of manganese oxide nanoparticles for adsorptive removal of malachite green from surface water. *Environmental Science and Pollution Research*, 30(10), 2023, pp.28144-28161. <https://doi.org/10.1007/s11356-022-24199-8>
- [5] Idriss, H., 2021. Decolorization of malachite green in aqueous solution via MgO nanopowder. *J. Optoelectron. Biomed. Mater*, 13(4), pp.183-192. <https://doi.org/10.15251/JOBM.2021.134.183>
- [6] Kandisa, R.V and Saibaba K.N., Dye Removal by Adsorption: A Review *J. Bioremediation Biodegrade*. 7, 2016, pp. 371-381. <https://doi.org/10.4172/2155-6199.1000371>
- [7] Kim, M., Sharma, N., Chung, J. and Yun, K. Activated graphene with fractal structure for the adsorption of malachite green with high removal rate. *Microporous and Mesoporous Materials*, 322, 2021, pp.11116-11139. <https://doi.org/10.1016/j.micromeso.2021.111166>
- [8] Lin, C., Wang, D., & Chen, H., 2022. Surface-Modified Magnesia Nanoparticles for the Removal of Organic Dyes from Wastewater: Experimental Insights. *Journal of Environmental Chemistry*, 18(2), pp.102-115.